Vertex renormalization of weak interactions and Cooper-pair breaking in cooling compact stars

Armen Sedrakian,[1,2] Herbert Müther,[1] and Peter Schuck[3]
[1]*Institute for Theoretical Physics, Tübingen University, D-72076 Tübingen, Germany*
[2]*Institute for Theoretical Physics, J. W. Goethe University, D-60438 Frankfurt-Main, Germany*
[3]*Groupe de Physique Théorique, Institut de Physique Nucléaire, F-91406 Orsay, France*
(Received 17 November 2006; revised manuscript received 21 May 2007; published 26 November 2007)

Below the critical temperature of superfluid phase transition baryonic matter emits neutrinos by breaking and recombination of Cooper pairs formed in the condensate. The weak vector and axial-vector vertices and the neutrino loss rates via pair breaking are modified by strong interactions in nuclear medium. We study these modifications nonperturbatively by summing infinite series of particle-hole loops in S-wave superfluid neutron matter. The interactions in the particle-hole channel are described within the Landau Fermi-liquid framework with the Landau parameters derived from the microscopic theory. The S-wave superfluid is described within the BCS theory. We derive the renormalized three-point vector and axial-vector vertices and the complete polarization tensor of matter and its low momentum transfer expansion. The leading-order term in this expansion and the associated neutrino losses arise at $O(q^2)$, consistent with the f-sum rule. The neutrino emission rate due to the pair breaking is parametrically suppressed compared to its one-loop counterpart by the ratio of the neutron recoil energy to the temperature, which is of order 5×10^{-3}. The approximations to the normal and anomalous self-energies that guarantee the conformity of the theory with the generalized Ward identities are established.

DOI: 10.1103/PhysRevC.76.055805 PACS number(s): 97.60.Jd, 26.60.+c, 21.65.+f, 13.15.+g

I. INTRODUCTION

Pair-correlated baryonic matter in compact stars emits neutrinos via the weak neutral current processes of pair breaking and recombination [1,2]

$$\begin{aligned} \{NN\} &\to N + N + \nu_f + \bar{\nu}_f, \\ N + N &\to \{NN\} + \nu_f + \bar{\nu}_f, \end{aligned} \tag{1}$$

where $\{NN\}$ refers to a Cooper pair, $N + N$ to two quasiparticle excitations, and ν_f and $\bar{\nu}_f$ to the neutrino and antineutrino of flavor f. The process (1) is limited to the temperature domain $T^* \leqslant T \leqslant T_c$, where T_c is the critical temperature of pairing phase transition and $T^* \sim 0.2T_c$. At and above T_c this reaction cannot occur, because momentum and energy cannot be conserved simultaneously in a process $N \to N + \nu_f + \bar{\nu}_f$, i.e., an on-mass-shell fermion cannot produce bremsstrahlung (in the absence of external gauge fields). At asymptotically low temperatures, $T \leqslant T^*$, the rate of the process (1) is exponentially small because the number of excitations out of the condensate is suppressed as $\exp(-\Delta/T)$, where $\Delta(T)$ is the gap in the quasiparticle spectrum.

Cooling simulations of neutron stars revealed the efficiency of the processes (1) in refrigerating their baryonic interiors from temperatures $T \leqslant T_c \sim 10^9$ K down to temperatures of order of 10^8 K [3–6]. The temperature domain above corresponds to the *neutrino cooling era* that spans the time domain $10^2 \leqslant t \leqslant 10^5$ years. The predicted surface temperatures of neutron stars during this and the following *photon cooling era* (where the star loses its thermal energy by emission of photons from the surface) are sensitive to the neutrino emission rates within this time domain. Remarkably, the process (1) relates the cooling rate of a compact star to the microscopic physics of its interiors and is sensitive to the density-temperature phase diagram of paired baryonic matter. Therefore, the measurements of surface (photon) luminosities of neutron stars and their interpretation in terms of cooling simulations have predictive power for analyzing the phase diagram and composition of baryonic matter [7–10].

The rate of the process (1) was initially computed in Refs. [1,2] in the case where the pairing interaction is in the $^1S_0$ partial wave, i.e., nucleons are paired in a spin-0, isospin-1 state. The influence of electric charge carried by proton Cooper pairs and the case of pairs forming a spin-1 superfluid were studied subsequently in Refs. [11]. In propagator language these rates correspond to the *one-loop* approximation to the polarization tensor of baryonic matter [2,10]. It has been known for a long time that to preserve the gauge invariance of the theory and the Ward identities one needs to sum up an infinite series of loop diagrams in the particle-hole channel. Independent of the nature of driving perturbations (e.g., density, spin, etc.) these summations are collectively known as the random-phase approximation (RPA) [12–16]. The summations of infinite series of loops can be cast into effective vertex functions that replace the bare vector and axial-vector vertices in the one-loop polarization tensor. The study of these vertex corrections to neutrino interactions in compact stars is in the beginning. For example, Ref. [17] carried out RPA summations in neutron and quark matter within the kinematical regime corresponding to neutrino scattering. Reference [18] applied the gauge invariance and vertices derived by Nambu [12] to the pair-breaking neutrino emission processes in the vector channel and concluded that the one-loop rate is suppressed by a factor $(v_F/c)^4$, where v_F is the baryon Fermi velocity.

In this article we set up a microscopic formalism for computing the vertex corrections to weak reaction rates that arise due to the strong interactions in baryonic matter. We consider the case of neutron matter at subnuclear densities, which we describe within the Landau Fermi-liquid theory derived from microscopic interactions. At these densities

neutron matter is characterized by an isotropic order parameter arising form the interaction in the $^1S_0$ partial wave channel; we solve the corresponding problem of pairing in the framework of the Bardeen-Cooper-Schrieffer (BCS) theory. In the nonrelativistic limit, the vector and axial-vector weak vertices are associated with scalar and spinor perturbations. Thus, the problem of renormalization of the weak vertices requires knowledge of the effective three-point vertices in the scalar and spin channels. At this point the theory of renormalization of weak vertices in baryonic matter makes contact with the theory of collective excitations in superfluid Fermi liquids, whose low-frequency, long-wavelength modes emerge as solutions of the RPA equations [13–16].

We apply the derived renormalized vertices to the neutrino-emission process in Eq. (1). Our derived rate differs from the one obtained in Ref. [18] due to a number of reasons. The renormalized vertices implemented in Ref. [18] were derived within a zero-temperature theory [12]; herein the polarization tensor *and* the vertices are derived within a finite temperature theory. This guarantees that the unitarity of the S matrix in the quantum mechanical process of bremsstrahlung is preserved. Reference [18] expands the matrix elements in powers of v_F/c and the leading-order contribution to the rate is $O(v_F^4/c^4)$; below we shall expand the polarization tensor with respect to small momentum transfer, q, and the leading-order contribution will arise at $O(q^2)$ [19]. As a consequence, we find a suppression of the neutrino emissivity which is by several orders of magnitude less than predicted in Ref. [18]. A comparison with the competing modified bremsstrahlung process [20–25] $N + N \to N + N + \nu_f + \bar{\nu}_f$, carried out in Ref. [26], shows that the pairing braking process in S-wave superfluids remains a potentially viable mechanism of cooling of neutron stars.

The article is organized as follows. In Sec. II we determine the quasiparticle spectrum in the paired state by solving the gap equation. We further compute the effective interactions (Landau parameters). Section III discusses the shortcomings of the one-loop polarization tensor. We compute the effective vector and axial-vector vertices by summing the particle-hole ladders in superfluid neutron matter in Sec. IV. The full polarization tensor that includes the vertex corrections is derived in Sec. V. We derive the generalized Ward identities for superfluid systems and discuss the conditions under which the theory preserves these identities in Sec. VI. Section VII is devoted to the computation of neutrino emissivity due to the pair-breaking process. Our conclusions are summarized in Sec. VIII. Some technical details are relegated to the Appendix.

II. *S*-WAVE PAIR-CONDENSATION IN NEUTRON MATTER

In this section we describe the neutron pair-condensate at subnuclear densities within the framework of the Fermi-liquid theory, which assumes that the elementary degrees of freedom are quasiparticles with a well-defined momentum-energy relation and infinite lifetime. The interactions between the quasiparticles are then described in terms of Landau parameters that depend on the momentum transfer (or scattering angle). Because the scattering angles involved are typically small, the momentum dependence of Landau parameters can be approximated by leading terms of their expansion in Legendre polynomial with respect to the scattering angle. The problem of pairing in neutron matter will be solved below within the BCS approximation, where the anomalous self-energy (the gap function) is computed from the bare interaction, whereas the normal self-energy is computed within the decoupling approximation, which ignores the effects of pair correlations on the single-particle spectrum of quasiparticles. A number of factors, such as the renormalization of the pairing interaction [27–36] and the wave-function renormalization [33,37,38], affect the absolute value of the gap. The role of these factors has not been settled yet, and we shall employ below the standard BCS approach, which has led to convergent and verifiable results for neutron matter (see the reviews in Refs. [39–41]).

Because the baryonic component of stellar matter is in thermal equilibrium to a good approximation, we shall use below the Matsubara Green's functions [42]. In the case of $^1S_0$ pairing these are defined as

$$\hat{G}_{\sigma\sigma'}(\boldsymbol{p},\tau) = -\delta_{\sigma\sigma'}\langle T_\tau \psi_{p\sigma}(\tau)\psi^\dagger_{p\sigma'}(0)\rangle, \tag{2}$$

$$\hat{F}_{\sigma\sigma'}(\boldsymbol{p},\tau) = \langle T_\tau \psi_{-p\downarrow}(\tau)\psi_{p\uparrow}(0)\rangle, \tag{3}$$

$$\hat{F}^\dagger_{\sigma\sigma'}(\boldsymbol{p},\tau) = \langle T_\tau \psi^\dagger_{p\uparrow}(\tau)\psi^\dagger_{-p\downarrow}(0)\rangle, \tag{4}$$

where $\sigma = \uparrow, \downarrow$ stands for spin (isospin indices are suppressed), τ is the imaginary time, T_τ is the imaginary time ordering symbol, and $\psi^\dagger_{p\sigma}(\tau)$ and $\psi_{p\sigma}(\tau)$ are the creation and destruction operators. In the momentum representation the propagators are given by

$$\hat{G}_{\sigma\sigma'}(ip_n,\boldsymbol{p}) = \delta_{\sigma\sigma'}\left(\frac{u_p^2}{ip_n-\epsilon_p}+\frac{v_p^2}{ip_n+\epsilon_p}\right), \tag{5}$$

$$\hat{F}_{\sigma\sigma'}(ip_n,\boldsymbol{p}) = -i\sigma_y u_p v_p\left(\frac{1}{ip_n-\epsilon_p}-\frac{1}{ip_n+\epsilon_p}\right), \tag{6}$$

and $F^\dagger_{\sigma\sigma'}(ip_n,\boldsymbol{p}) = F_{\sigma\sigma'}(ip_n,\boldsymbol{p})$, where $p_n = (2n+1)\pi T$ is the fermionic Matsubara frequency, σ_y is the y component of the Pauli matrix, $u_p^2 = (1/2)(1+\xi_p/\epsilon_p)$ and $v_p^2 = 1-u_p^2$ are the Bogolyubov amplitudes and

$$\epsilon_p = \sqrt{\xi_p^2+\Delta_p^2} \tag{7}$$

is the quasiparticle spectrum, where $\xi_p = p^2/2m + \mathrm{Re}\Sigma(p) - \mu$ is the spectrum in the unpaired state and m and μ are the bare mass and the chemical potential. Here $\Sigma(p)$ and $\Delta(p)$ are the normal and anomalous self-energies. For the later diagrammatic analysis we shall need the hole propagator, which is given by

$$\begin{aligned}\hat{G}^\dagger_{\sigma\sigma'}(ip_n,\boldsymbol{p}) &= \hat{G}_{\sigma\sigma'}(-ip_n,-\boldsymbol{p})\\ &= -\delta_{\sigma\sigma'}\left(\frac{u_p^2}{ip_n+\epsilon_p}+\frac{v_p^2}{ip_n-\epsilon_p}\right).\end{aligned} \tag{8}$$

The spin dependence of propagators for S-wave spin-0 and isospin-1 pairing is given by $\hat{G}_{\sigma\sigma'}(ip_n,\boldsymbol{p}) = \delta_{\sigma\sigma'}G(ip_n,\boldsymbol{p})$ and $\hat{F}_{\sigma\sigma'}(ip_n,\boldsymbol{p}) = -i\sigma_y F(ip_n,\boldsymbol{p})$.

Because the quasiparticles are confined to the vicinity of the Fermi surface we expand the normal self-energy around the Fermi momentum, p_F, to obtain

$$\xi(p) \simeq v_F(p - p_F) - \mu^*, \tag{9}$$

where $\mu^* \equiv -p_F^2/2m + \mu - \mathrm{Re}\Sigma(p_F)$ is the effective chemical potential, $v_F = p_F/m^*$ is the Fermi velocity, and $m^* = m[1 + (m/p_F)\partial_p \mathrm{Re}\Sigma(p)|_{p=p_F}]^{-1}$ is the effective mass. The dependence of self-energies on the off-mass shell energy will be neglected, i.e., the wave-function renormalization is set to unity. The anomalous self-energy in the BCS mean-field approximation is given by

$$\Delta(p) = \int \frac{d^3p'}{2(2\pi)^3} V(p, p') \frac{\Delta(p')}{\sqrt{\xi(p')^2 + \Delta(p')^2}} \times [1 - 2f(\epsilon(p'))], \tag{10}$$

where $V(p, p')$ is the bare interaction in the ${}^1S_0$ partial wave channel and the finite-temperature effects are contained in the Fermi distribution function $f(\epsilon_p) = [1 + \exp(\epsilon_p/T)]^{-1}$. The gap equation is supplemented by the equation for the density

$$\rho = \int \frac{d^3p}{(2\pi)^3} \{u_p^2 f(\epsilon_p) + v_p^2[1 - f(\epsilon_p)]\}, \tag{11}$$

which determines the chemical potential in a self-consistent manner. Figure 1 shows the temperature dependence of the ${}^1S_0$ pairing gap in neutron matter for several densities parameterized in terms of the Fermi wave number, $k_F = (3\pi^2\rho)^{1/3}$. The gap at zero temperature and the critical temperature for unpairing are listed in the Table I. The dependence of ratio $\Delta(T)/T$ on T/T_c is nonuniversal in our model, i.e., contrary to the prediction of the BCS theory with contact pairing interaction, it depends on the density.

Within the adopted Fermi-liquid description of neutron matter, the particle-hole interaction is given by

$$V^{\mathrm{ph}}(\boldsymbol{q}) = v^V(\boldsymbol{q}) + v^A(\boldsymbol{q})(\boldsymbol{\sigma} \cdot \boldsymbol{\sigma}'), \tag{12}$$

where $\boldsymbol{\sigma}$ is the Pauli matrix. The Landau parameters $v^V(\boldsymbol{q})$ and $v^A(\boldsymbol{q})$ depend on the momentum transfer $\boldsymbol{q}$ in the process where both fermion momenta are on the Fermi surface [43]. The tensor and spin-orbit terms are small in neutron matter and were neglected in Eq. (12). The full dependence of these parameters on the momentum transfer is commonly approximated by a Legendre polynomial with respect to the angle formed by the incoming fermions, whereby only the leading and next-to-leading-order terms contribute significantly.

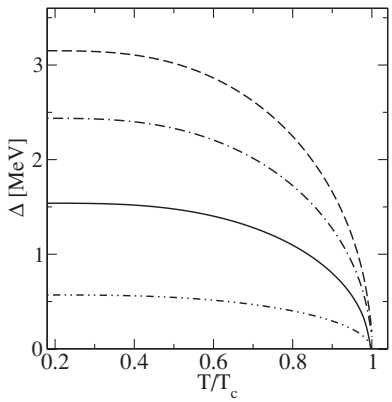

FIG. 1. Temperature dependence of the ${}^1S_0$ pairing gap in neutron matter for Fermi wave vectors $k_F = 0.4$ (solid line), 0.8 (dashed line), 1.2 (dashed-dotted line), and 1.6 (dashed-double-dotted line).

TABLE I. Density dependence of the effective mass, the scalar and spin-spin interactions, the pairing gap, and the critical temperature; the interactions are given in units of the density of states $\nu(p_F)$.

p_F (fm^{-1})	m^*/m	v^V	v^A	$\Delta(p_F)$ (MeV)	T_c (MeV)
0.4	1.02	−0.56	0.55	1.54	0.85
0.6	1.00	−0.50	0.49	2.60	1.44
0.8	0.97	−0.47	0.44	3.15	1.78
1.0	0.94	−0.45	0.41	3.09	1.80
1.2	0.92	−0.43	0.40	2.44	1.46
1.4	0.88	−0.41	0.40	1.41	0.88
1.6	0.84	−0.36	0.39	0.57	0.38

Table I lists the effective mass and the zeroth-order Landau parameters in the scalar and spin channels computed within the formalism of Ref. [44] starting from the CD Bonn potential [45]. Because the Landau parameters were derived from the Bruckner G matrix, they do not fulfill the Landau sum rule. The sum rule could be restored, if the Landau parameters are computed from an interaction that includes, in addition to the direct interaction, the so-called induced interaction. However, induced interactions include the class of particle-hole ladder diagrams that we will sum up in Sec. IV, and for that purpose the driving term can include only summations in the particle-particle channel. The solution of the gap equation was obtained by applying the iterative method with a "running" cutoff [46] whereby the effective pairing interaction was approximated by the Gogny DS1 force [47].

III. POLARIZATION TENSOR AT ONE-LOOP

The polarization tensor of baryons at one-loop is shown in Fig. 2 and is given analytically by

$$\Pi^{V/A}(q) = T \sum_{\sigma,p} [G(p)G(p+q) \mp F(p)F^\dagger(p+q)], \tag{13}$$

where $p = (ip_0, \boldsymbol{p})$. The upper/lower signs correspond to vector current (V) and axial-vector current (A) couplings. In writing Eq. (13) we assumed that baryons carry the same isospin quantum number. Performing the Matsubara sums in

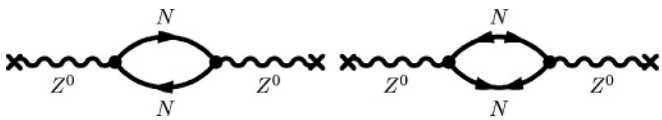

FIG. 2. The one-loop contribution to the polarization tensor in the superfluid matter; solid lines refer to the baryon propagators and wavy lines to the (amputated) Z^0 propagator.

Eq. (13) (see the Appendix) we obtain

$$\Pi^{V/A}(q) = \sum_{\sigma \boldsymbol{p}} [f(\epsilon_p) - f(\epsilon_k)] \left(\frac{A_\mp}{iq + \epsilon_p - \epsilon_k} - \frac{B_\mp}{iq - \epsilon_p + \epsilon_k} \right) + \sum_{\sigma \boldsymbol{p}} [f(-\epsilon_p) - f(\epsilon_k)] \left(\frac{C_\mp}{iq - \epsilon_k - \epsilon_p} - \frac{D_\mp}{iq + \epsilon_p + \epsilon_k} \right), \quad (14)$$

where $k = p + q$, $A_\mp = u_p^2 u_k^2 \mp h$, $B_\mp = v_p^2 v_k^2 \mp h$, $C_\mp = u_k^2 v_p^2 \pm h$, $D_\mp = u_p^2 v_k^2 \pm h$, and $h = u_p u_k v_p v_k$. We are interested in the imaginary part of the polarization tensor that after analytical continuation in Eq. (14) becomes [note that $f(-\epsilon_p) = 1 - f(\epsilon_p)$]

$$\Im\mathrm{m}\,\Pi^{V/A}(q) = -\pi \sum_{\sigma \boldsymbol{p}} [f(\epsilon_p) - f(\epsilon_k)](A_\mp + B_\mp)\delta(\omega + \epsilon_p - \epsilon_k) - \pi \sum_{\sigma \boldsymbol{p}} [f(-\epsilon_p) - f(\epsilon_k)][C_\mp \delta(\omega - \epsilon_p - \epsilon_k) - D_\mp \delta(\omega + \epsilon_p + \epsilon_k)]. \quad (15)$$

To obtain the first line we used the fact that the quasiparticle spectra are invariant under spatial reflections, i.e., $\epsilon(-\boldsymbol{p}) = \epsilon(\boldsymbol{p})$. The first line in Eq. (15) corresponds to the process of scattering where a quasiparticle is promoted out of the condensate into an excited state or an excitation merges with the condensate. The corresponding piece of the response function $\Im\mathrm{m}\Pi^{V/A}(q)$ vanishes for small momentum transfers. Indeed neutrino energies are of order of temperature, i.e., their wave vectors $q[\mathrm{fm}^{-1}] \sim \omega_\nu/\hbar c \sim T/\hbar c \sim 1/197.3 \ll 1$. However, the neutron wave vectors $\sim k_F \sim 1\ \mathrm{fm}^{-1}$. On expanding the argument of the δ function with respect to small $|\boldsymbol{q}|$ one finds

$$\omega - q\,\frac{\xi_p}{\epsilon_p}\frac{\partial \xi_{p+q}}{\partial q}\bigg|_{q=0} - q\,\frac{\Delta_p}{\epsilon_p}\frac{\partial \Delta_{p+q}}{\partial q}\bigg|_{q=0} = 0. \quad (16)$$

If we assume that $\Delta \neq \Delta(p)$, the third term on the left-hand side vanishes. It follows that $x \equiv (\boldsymbol{p}\cdot\boldsymbol{q})/pq = (\epsilon_p/\xi_p)(\omega/vq) \leqslant 1$, where $v(\sim v_F)$. For on mass-shell neutrinos $\omega = cq$ and the latter condition cannot be satisfied. The nonlocality of the gap function in the momentum or frequency domains will alter this conclusion, but an assessment of its importance requires a specific model of momentum and frequency dependence of the gap function (for S-wave interactions the momentum and energy dependences are described, respectively, in Refs. [38,47–49] and [33,35,37]). The second line in Eq. (15) describes the process of pair breaking and recombination, i.e., excitation of pairs of quasiparticles out of the condensate and restoration of a pair within the condensate. Because we are interested in the emission process we shall keep only the terms that do not vanish for $\omega > 0$; then, the pair-breaking contribution is given by

$$\Im\mathrm{m}\,\Pi^{V/A}(q) = -\pi \sum_{\sigma \boldsymbol{p}} [f(-\epsilon_p) - f(\epsilon_k)]C_\mp. \quad (17)$$

In the limit $\boldsymbol{q} \to 0$ and assuming that $\Delta \neq \Delta(p)$ the integrations in Eq. (17) can be performed analytically. For the imaginary part of vector current response one finds

$$\Im\mathrm{m}\,\Pi^V(q) = -2\pi\, \nu(p_F) g(\omega)^{-1} f \left(\frac{\omega}{2}\right)^2 \times \left(\frac{\Delta^2}{\omega^2}\right) \frac{\omega}{\sqrt{\omega^2 - 4\Delta^2}} \theta(\omega - 2\Delta), \quad (18)$$

where $\nu(p_F) = m^* p_F/2\pi^2$ is the density of states ($\hbar = 1$) and θ is the Heaviside step function. Note the threshold behavior of the vector current response, which is finite for frequencies that are large compared to 2Δ-the energy needed to break a pair.

IV. WEAK INTERACTION VERTICES

We now consider the weak vector and axial-vector vertices in the nuclear medium featuring a condensate. Because the particle-hole interactions in the medium (which are represented by the Landau parameters, see Table I) are not small, vertex renormalizations require summations of infinite number of particle-hole loops. There are four topologically nonequivalent vertices in the superfluid state in general. As we shall see, the particle-hole symmetry reduces their number by one. Because neutrons pair in an isospin-1 state (neutron-proton pairing is unimportant for large asymmetries [50]) we shall suppress the isospin indices. The expansion of the Landau parameters in Legendre polynomials will be truncated at the leading order (the next-to-leading-order terms are suppressed by powers of v_F/c). Thus, the particle-hole interaction is approximately given by

$$V^{\mathrm{ph}} \simeq v^V + v^A(\boldsymbol{\sigma}\cdot\boldsymbol{\sigma}'). \quad (19)$$

The integral equation defining the effective weak vertices, which we write in an operator form, are given by

$$\hat{\Gamma}_1^a = \Gamma_0^a + v^a\big(G\Gamma_1^a G + \hat{F}\hat{\Gamma}_3^a G + G\hat{\Gamma}_2^a\hat{F} + \hat{F}\Gamma_4^a\hat{F}\big), \quad (20)$$

$$\hat{\Gamma}_2^a = v^a\big(G\hat{\Gamma}_2^a G^\dagger + \hat{F}\Gamma_4^a G^\dagger + G\Gamma_1^a\hat{F} + \hat{F}\hat{\Gamma}_3^a\hat{F}\big), \quad (21)$$

$$\hat{\Gamma}_3^a = v^a\big(G^\dagger\hat{\Gamma}_3^a G + \hat{F}\Gamma_1^a G + G^\dagger\Gamma_4^a\hat{F} + \hat{F}\hat{\Gamma}_2^a\hat{F}\big), \quad (22)$$

and are displayed diagrammatically in Fig. 3. Here $\hat{F} = -i\sigma_y F$, v^a with $a \in V$, A are defined in Eq. (19), $\Gamma_0^V = 1$ and $\Gamma_0^A = \boldsymbol{\sigma}$. The fourth integral equation for the vertex Γ_4^a follows on interchanging particle and hole propagators $G \leftrightarrow G^\dagger$ in Eq. (20). The momentum space representation of operator equation (20) is given by

$$\hat{\Gamma}_1^a(q) = \Gamma_0^a + v^a \int \frac{d^4p}{(2\pi)^4}\big[G(p)\Gamma_1^a(q)G(p+q) + G(p)\Gamma_2^a(q)\hat{F}(p+q) + \hat{F}(p)\Gamma_3^a(q)G(p+q) + \hat{F}(p)\Gamma_4^a(q)\hat{F}(p+q)\big]. \quad (23)$$

The momentum space expressions for Eqs. (21) and (22) are analogous to the one given above. Even though the driving interactions are local in time, the summations at finite temperatures lead to time-retarded interactions, which imply that the effective vertices in Eqs. (20)–(22) are complex in general. Considering the scalar interaction Γ_0^V we obtain

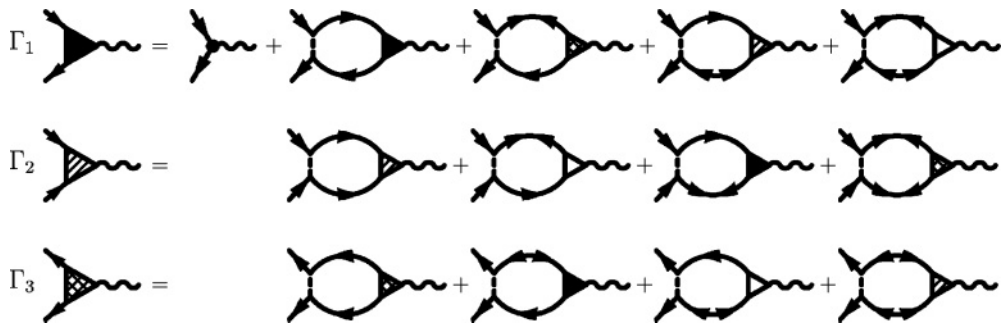

FIG. 3. Coupled integral equations for the effective weak vertices in superfluid baryonic matter. The "normal" Γ_1 vertex (full triangle) and two "anomalous" vertices Γ_2 (hatched) and Γ_3 (shaded triangle) are shown explicitly, the fourth vertex (empty triangle) is obtained by interchanging the particle and hole lines in the first line. The anomalous vertices vanish in the normal state.

$$v^V \begin{pmatrix} (v^V)^{-1} - [\Pi_{GG}(q) - \Pi_{FF}(q)] & \Pi_{GF}(q) & \Pi_{FG}(q) \\ -2\Pi_{GF}(q) & (v^V)^{-1} - \Pi_{GG^\dagger}(q) & \Pi_{FF}(q) \\ -2\Pi_{FG}(q) & \Pi_{FF}(q) & (v^V)^{-1} - \Pi_{G^\dagger G}(q) \end{pmatrix} \begin{pmatrix} \Gamma_1^V(q) \\ \Gamma_2^V(q) \\ \Gamma_3^V(q) \end{pmatrix} = \begin{pmatrix} \Gamma_0^V \\ 0 \\ 0 \end{pmatrix}, \tag{24}$$

where

$$\Pi_{XX'}(q) = \int \frac{d^3p}{(2\pi)^3} L_{XX'}(q, \boldsymbol{p}) = \int \frac{d^3p}{(2\pi)^3} \sum_{ip} X(p)X'(p+q), \tag{25}$$

and $X, X' \in G, F, G^\dagger$ (see the Appendix). The symmetries among the loops $L_{GG} = L_{G^\dagger G^\dagger}$, $L_{GF} = L_{FG^\dagger}$, and $L_{FG} = L_{G^\dagger F}$ imply that $\Gamma_1^V = \Gamma_4^V$ and $\Gamma_1^A = -\Gamma_4^A$. For energy-momentum independent interactions the integral equation (24) reduces to three coupled linear equations for the complex functions Γ_i^V, $i = 1, 2, 3$. The details of the computation of the coefficients in Eqs. (24) are relegated to the Appendix. In the weak-coupling BCS limit there exist *approximate* symmetry among the loops

$$L_{GF} = -L_{FG}, \quad L_{G^\dagger G} = L_{GG^\dagger}, \tag{26}$$

which allow us to reduce the number of equations in the set (24) from three to two. The relations (26) are exact at the threshold $\omega = 2\Delta$ and hold approximately for systems with strong degeneracy (corrections being suppressed by powers of the ratio of temperature over the Fermi energy). It follows then from Eq. (24) that $\Gamma_2^V = -\Gamma_3^V$. The solutions for the remaining vertices Γ_1 and Γ_2 are convenient to express through linear combinations of the polarization tensors (25), defined as

$$\mathcal{A}(q) = \Pi_{GG}(q) - \Pi_{FF}(q) = \int \frac{d^3p}{(2\pi)^3} \mathcal{F}_p^-(\boldsymbol{q}) \mathcal{G}_p(\omega, \boldsymbol{q}), \tag{27}$$

$$\mathcal{B}(q) = 2\Pi_{FG}(q) = -\omega\Delta \int \frac{d^3p}{(2\pi)^3} \frac{\mathcal{G}_p(\omega, \boldsymbol{q})}{\epsilon_p}, \tag{28}$$

$$\mathcal{C}(q) = \Pi_{GG^\dagger}(q) + \Pi_{FF}(q) - (v^V)^{-1} = \int \frac{d^3p}{(2\pi)^3} [2\epsilon_p \mathcal{G}_p(0,0) - \mathcal{F}_p^+(\boldsymbol{q}) \mathcal{G}_p(\omega, \boldsymbol{q})], \tag{29}$$

where $(\boldsymbol{k} = \boldsymbol{p} + \boldsymbol{q})$. To obtain the last equation we used the fact that

$$1 + v^V \int^\Lambda \frac{d^4p}{(2\pi)^4} (\Pi_{GG^\dagger} + \Pi_{FF}) \Big|_{\omega=0, \boldsymbol{q}=0} = 0, \tag{30}$$

where Λ is a three-dimensional ultraviolet cutoff on the momentum integration, which is required for regularization of the gap equation (30). Λ may be adjusted to reproduce the gaps obtained from finite range interactions in Sec. II. This is also needed to preserve the generalized Ward identities relating the Γ_2 vertex to the anomalous self-energy (see Sec. VI). The functions $\mathcal{F}$ and $\mathcal{G}$ in Eqs. (27)–(29) are given by

$$\mathcal{F}_p^\pm(\boldsymbol{q}) = \left(\frac{\epsilon_p + \epsilon_k}{2}\right) \left(1 \pm \frac{\xi_p \xi_k}{\epsilon_p \epsilon_k} + \frac{\Delta^2}{\epsilon_p \epsilon_k}\right), \tag{31}$$

$$\mathcal{G}_p(\omega, \boldsymbol{q}) = \frac{1 - f(\epsilon_p) - f(\epsilon_k)}{\omega^2 - (\epsilon_p + \epsilon_k)^2 + i\delta} - \frac{f(\epsilon_p) - f(\epsilon_k)}{\omega^2 - (\epsilon_p - \epsilon_k)^2 + i\delta}. \tag{32}$$

The two linear equations for the normal and anomalous vertices can be expressed through the functions in Eqs. (27)–(29) and solved to obtain

$$\Gamma_1^V(q) = \frac{\mathcal{C}(q)}{\mathcal{C}(q) - v^V[\mathcal{A}(q)\mathcal{C}(q) + \mathcal{B}(q)^2]}, \tag{33}$$

$$\Gamma_2^V(q) = -\frac{\mathcal{B}(q)}{\mathcal{C}(q) - v^V[\mathcal{A}(q)\mathcal{C}(q) + \mathcal{B}(q)^2]}. \tag{34}$$

Note that the vertices share the same complex poles that determine the collective modes of superfluid and their damping. The modes derived from the scalar driving interaction v^V correspond to the acoustic modes oscillations.

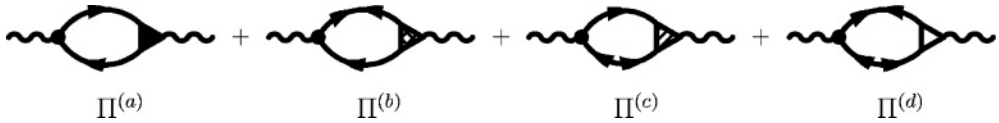

FIG. 4. The sum of polarization tensors that contribute to the neutrino emission rate. The contributions form $\Pi^{(b)}(q)$ and $\Pi^{(c)}(q)$ vanish at one loop.

V. THE FULL POLARIZATION TENSOR

Having determined the effective vertices $\Gamma_1^V(q)$ and $\Gamma_2^V(q)$, we now construct the complete polarization tensor, which is given diagrammatically in Fig. 4. The sum of the four contributions to the polarization tensor, shown in Fig. 4, is given by

$$\Pi^V(q) = \frac{\mathcal{A}(q)\mathcal{C}(q) + \mathcal{B}(q)^2}{\mathcal{C}(q) - v^V[\mathcal{A}(q)\mathcal{C}(q) + \mathcal{B}(q)^2]}. \tag{35}$$

Equation (35) is our central result valid for arbitrary momentum transfers. It can be used to compute the emissivity directly, but it is illuminating to work in the small $\boldsymbol{q}$ limit. To leading order, the full polarization tensor vanishes for $\boldsymbol{q} = 0$ (note that this is contrary to the one-loop polarization tensor, which is finite in this limit, see Eq. (14) and the following discussion.) Indeed, taking the limit $\boldsymbol{q} \to 0$ in Eqs. (27)–(29) and substituting in Eq. (35) we find that

$$\lim_{\boldsymbol{q}\to 0} \Pi^V(\boldsymbol{q}, \omega) = 0. \tag{36}$$

This result is consistent with the f-sum rule [51]

$$\lim_{\boldsymbol{q}\to 0} \int d\omega\, \omega\, \mathrm{Im}\, \Pi^V(\boldsymbol{q}, \omega) = 0, \tag{37}$$

which follows directly from Eq. (36). The opposite need not to be true for arbitrary functional dependence of $\mathrm{Im}\Pi^V(\boldsymbol{q}, \omega)$ on frequency but is the case in practice. The reason is that for causal processes polarization tensors are odd functions of frequency. Furthermore, because they should correspond to stable collective modes the condition $\omega\, \mathrm{Im}\Pi^V(\boldsymbol{q}, \omega) \geqslant 0$ is satisfied, which, combined with the f-sum rule, leads back to Eq. (36).

Consider now the next-to-leading-order terms. Keeping only the leading order piece of function $\mathcal{F}_p^{\pm}(\boldsymbol{q})$ in Eqs. (27) and (29), i.e. $\mathcal{F}_p^{\pm}(0)$, one finds that the polarization function vanishes order by order in the expansion of the function $\mathcal{G}_p(\omega, \boldsymbol{q})$; thus instead of straightforward expansions of kernels in Eqs. (27)–(29), we shall expand only the functions $\mathcal{F}_p^{\pm}(\boldsymbol{q})$:

$$\mathcal{F}_p^{+}(\boldsymbol{q}) = \left(\frac{\epsilon_p + \epsilon_k}{2}\right)\left(1 + \frac{\xi_p\xi_k}{\epsilon_p\epsilon_k} + \frac{\Delta^2}{\epsilon_p\epsilon_k}\right) \simeq 2\epsilon_p + \frac{\xi_p\xi_q^0}{\epsilon_p} \tag{38}$$

and

$$\mathcal{F}_p^{-}(\boldsymbol{q}) = \left(\frac{\epsilon_p + \epsilon_k}{2}\right)\left(1 - \frac{\xi_p\xi_k}{\epsilon_p\epsilon_k} + \frac{\Delta^2}{\epsilon_p\epsilon_k}\right) \simeq \frac{2\Delta^2}{\epsilon_p} - \frac{\Delta^2\xi_p\xi_q^0}{\epsilon_p^3}, \tag{39}$$

where $\xi_q^0 = q^2/2m$ is the nucleon recoil energy (the linear in q terms are omitted because they vanish on angle integrations). Substituting these expressions back into Eqs. (27)–(29) one finds

$$\mathcal{A}(q) = -\Delta^2\xi_q^0 I_A(q) + 2\Delta^2 I_B(q), \tag{40}$$

$$\mathcal{B}(q) = -\omega\Delta I_B(q), \tag{41}$$

$$\mathcal{C}(q) = \xi_q^0 I_C(q) - \frac{\omega^2}{2} I_B(q), \tag{42}$$

where we defined the following integrals

$$I_A(q) = \int \frac{d^3p}{(2\pi)^3}\frac{\xi_p}{\epsilon_p^3}\mathcal{G}_p(\omega, \boldsymbol{q}), \tag{43}$$

$$I_B(q) = \int \frac{d^3p}{(2\pi)^3}\frac{1}{2\epsilon_p}\mathcal{G}_p(\omega, \boldsymbol{q}), \tag{44}$$

$$I_C(q) = \int \frac{d^3p}{(2\pi)^3}\frac{\xi_p}{\epsilon_p}\mathcal{G}_p(\omega, \boldsymbol{q}). \tag{45}$$

The pole(s) of the polarization tensor (or equivalently of the vertex function) on the real axis determine the dispersion relation of the collective excitations, i.e.

$$\mathrm{Re}\mathcal{D}(q) = \mathrm{Re}\mathcal{C}(q) - v^V\mathrm{Re}[\mathcal{A}(q)\mathcal{C}(q) + \mathcal{B}(q)^2] = 0. \tag{46}$$

Substituting Eqs. (40)–(42) we obtain the dispersion relation for the acoustic modes to the leading $O(q^2)$ order $\omega^2 = c^2q^2$, where the sound velocity is defined as

$$c^2 = \frac{1}{m^*\mathrm{Re}\, I_B}[\mathrm{Re}I_C - 2v^V\Delta^2\mathrm{Re}(I_B\, I_C)]. \tag{47}$$

At the next-to-leading order in small-q expansion the polarization tensor is given by

$$\Pi_1^V(q) = \mathcal{A}_1(q) + \frac{\mathcal{A}_0(q)}{\mathcal{C}_0(q)}\mathcal{C}_1(q) = -\Delta^2\xi_q^0\left[I_A(q) + \frac{4}{\omega^2}I_C(q)\right], \tag{48}$$

where the subscripts 0 and 1 refer to the leading and next-to-leading-order terms of the expansion. It is sufficient to evaluate the integrals on the right-hand side in the limit $q = 0$ at the order we are working and the imaginary part of the polarization tensor can be evaluated analytically

$$\Im\mathrm{m}\Pi_1(\omega) = -8\pi\nu(p_F)\frac{\Delta^2\xi_q^0}{\omega^3}g(\omega)^{-1}f\left(\frac{\omega}{2}\right)^2\theta(\omega - 2\Delta). \tag{49}$$

It is instructive to compare the latter result with the one-loop polarization tensor in the limit $\boldsymbol{q} = 0$ given by Eq. (18). Apart from factors of order of unity, these two results differ by the ratio ξ_q^0/ω, which the parameter characterizing the suppression

of the full polarization function compared to its one-loop counterpart. Because $\omega \sim |\boldsymbol{q}| \sim T$, this parameter translates into T/m^*.

VI. GENERALIZED WARD IDENTITIES

In this section we discuss the consistency between the weak interaction vertices and the self-energies on the basis of generalized Ward identities [13,15]. Consider local gauge transformations of the operators (spin indices are suppressed in this section)

$$\psi'(x) = \psi(x)e^{if(x)}, \quad \psi^{\dagger\prime}(x) = \psi^\dagger(x)e^{-if(x)}. \tag{50}$$

These transformations are equivalent to application of a field $\partial f/\partial x_i$, $i = 0, 1, 2, 3$, where $x_0 = \tau$ is the (imaginary) time component and $\boldsymbol{x} = x_\alpha$, $\alpha = 1, 2, 3$, is the spatial component of the four-vector x. The change in the Green's functions induced by the gauge transformation above is

$$\begin{aligned}\delta G(x_1, x_2) &= G'(x_1, x_2) - G(x_1, x_2)\\ &= if(x_1)G(x_1, x_2) - G(x_1, x_2)if(x_2), \qquad (51)\\ \delta F(x_1, x_2) &= F'(x_1, x_2) - F(x_1, x_2)\\ &= if(x_1)F(x_1, x_2) + F(x_1, x_2)if(x_2), \qquad (52)\end{aligned}$$

where the primed Green's functions are obtained from the unprimed ones by substitution (50) into their definition. In momentum representation and for a spatially homogeneous system one finds

$$\begin{aligned}\delta G(p, p+q) &= i[f(q)G(p) - G(p+q)f(q)], \qquad (53)\\ \delta F(p, p+q) &= i[f(q)F(p) + F(p+q)f(q)]. \qquad (54)\end{aligned}$$

However, the changes in the Green's functions can be obtained diagrammatically. The relevant diagrams for δG and δF are analogous to those in Fig. 3. They are obtained by a vertical cut through the propagators in each loop in Fig. 3 and subsequent removal of the left-hand side of the loop (formally this is equivalent to taking the derivative of each vertex Γ_i^a with respect to the driving interaction v^a). The result, written in the operator form, is given by

$$\delta G = \left[G\Gamma_1^i G + \hat{F}\hat{\Gamma}_3^i G + G\hat{\Gamma}_2^i\hat{F} + \hat{F}\Gamma_4^i\hat{F}\right]\frac{\partial f}{\partial x_i}, \tag{55}$$

$$\delta\hat{F} = \left[G\hat{\Gamma}_2^i G^\dagger + \hat{F}\Gamma_4^i G^\dagger + G\Gamma_1^i\hat{F} + \hat{F}\hat{\Gamma}_3^i\hat{F}\right]\frac{\partial f}{\partial x_i}, \tag{56}$$

where summation over repeated indices is assumed; here we dropped the channel index a, because we restrict the discussion to the scalar vertex, i.e., $v^a = v^V$.

On exploiting the symmetries among the loops, derived in the Appendix, these relations simplify to

$$\begin{aligned}\delta G(p, p+q) &= \left\{[G(p)G(p+q) - F(p)F(p+q)]\Gamma_1^i(q)\right.\\ &\quad \left. + 2F(p)G(p+q)\Gamma_2^i(q)\right\}iq_i f(q), \qquad (57)\\ \delta F(p, p+q) &= \left\{-2F(p)G(p+q)\Gamma_1^i + [G(p)G^\dagger(p+q)\right.\\ &\quad \left. + F(p)F(p+q)]\Gamma_2^i\right\}iq_i f(q). \qquad (58)\end{aligned}$$

Combining pairwise Eqs. (53), (57) and (54), (58) we obtain

$$\begin{aligned}&G(p) - G(p+q)\\ &\quad = \left\{[G(p)G(p+q) - F(p)F(p+q)]\Gamma_1^i(q)\right.\\ &\qquad \left. + 2F(p)G(p+q)\Gamma_2^i(q)\right\}q_i, \qquad (59)\\ &F(p) + F(p+q)\\ &\quad = \left\{-2F(p)G(p+q)\Gamma_1^i + [G(p)G^\dagger(p+q)\right.\\ &\qquad \left. + F(p)F(p+q)]\Gamma_2^i\right\}q_i. \qquad (60)\end{aligned}$$

The components of Eq. (24), with the approximation (26), can be written as

$$\begin{aligned}\Gamma_1(q) &= 1 + v^V[\Pi_{GG}(q) - \Pi_{FF}(q)]\Gamma_1(q) + v^V[\Pi_{FG}(q)\\ &\quad - \Pi_{GF}(q)]\Gamma_2(q), \qquad (61)\\ \Gamma_2(q) &= v^V[\Pi_{GG^\dagger}(q) + \Pi_{FF}(q)]\Gamma_2(q) + 2v^V\Pi_{GF}(q)\Gamma_1(q). \qquad (62)\end{aligned}$$

We now define the spatial parts of these vertex functions as the solutions to the equations

$$\begin{aligned}\Gamma_1(q) &= \frac{2\boldsymbol{p}+\boldsymbol{q}}{2m} + v^V\left[\Pi_{GG}(q) - \Pi_{FF}(q)\right]\Gamma_1(q)\\ &\quad + v^V\left[\Pi_{FG}(q) - \Pi_{GF}(q)\right]\Gamma_2(q), \qquad (63)\\ \Gamma_2(q) &= v^V\left[\Pi_{GG^\dagger}(q) + \Pi_{FF}(q)\right]\Gamma_2(q)\\ &\quad + 2v^V\Pi_{GF}(q)\Gamma_1(q), \qquad (64)\end{aligned}$$

and consider first the contraction $q_i\Gamma_1^i = q_0\Gamma_1 - \boldsymbol{q}\cdot\Gamma_1$. With the help of Eq. (59) we then obtain

$$\begin{aligned}q_i\Gamma_1^i(q) &= q_0 - \xi_{p+q} + \xi_p + v^V\left[\Pi_{GG}(q) - \Pi_{FF}(q)\right]q_i\\ &\quad \times\Gamma_1^i(q) + v^V\left[\Pi_{FG}(q) - \Pi_{GF}(q)\right]q_i\Gamma_2^i(q)\\ &= q_0 - \xi_{p+q} + \xi_p + v^V\sum_{ip}\int\frac{d^3p}{(2\pi)^3}\\ &\quad \times[G(p) - G(p+q)]\\ &= q_0 - \xi_{p+q} + \xi_p - \Omega(p_F+q) + \Omega(p_F)\\ &= G^{-1}(p+q) - G^{-1}(p), \qquad (65)\end{aligned}$$

where the self-energy is given by

$$\Omega(p_F) \equiv v^V\sum_{ip}\int^{\Lambda'}\frac{d^3p}{(2\pi)^3}G(p), \tag{66}$$

where the cutoff Λ' regularizes the ultraviolet divergence due to the contact form of the interaction. Consistency with the Ward identity, $q_i\Gamma_1^i = G^{-1}(p+q) - G^{-1}(p)$, requires $\Omega(p_F) = \Sigma(p_F)$, where the latter self-energy is implicitly defined by Eq. (9). This matching condition, and therefore the Ward identity, is violated because (i) the propagator in the kernel of Eq. (66) includes the pairing correlations, whereas the normal self-energy $\Sigma(p)$ is computed for $\Delta = 0$. This approximation, known as the decoupling approximation, is justified by the smallness of the gap compared to other scales involved, see Ref. [41]. (ii) The interaction term in the definition of $\Sigma(p)$ is commonly approximated by the two-body scattering T matrix, which is finite range, whereas the interaction v^V in Eq. (66) is zero-range. Because the cutoff Λ' is unspecified, it may be adjusted to reproduce the results

from finite range interactions. Note that the Ward identities for the scalar and vector components of the four-vector vertex Γ_1^i follow from the generalized Ward identity (65) on taking successively the limit $\boldsymbol{q} \to 0$ followed by $\omega \to 0$ (for the scalar vertex) and the limit $\omega \to 0$ followed by $\boldsymbol{q} \to 0$ (for the vector vertex).

We now derive the second Ward identity for the vertex Γ_2^i by utilizing Eq. (60). In analogy to the derivation of Eq. (65) we find

$$\begin{aligned} q_i \Gamma_2^i(q) &= v^V \left[\Pi_{GG^\dagger}(q) + \Pi_{FF}(q)\right] q_i \Gamma_2^i(q) \\ &\quad + 2 v^V \Pi_{GF}(q) q_i \Gamma_1^i(q) \\ &= v^V \sum_{ip} \int^\Lambda \frac{d^3p}{(2\pi)^3} [F(p+q) + F(p)] \\ &= \Delta(p_F) + \Delta(p_F + q), \end{aligned} \tag{67}$$

where the gap function

$$\Delta(p_F) = v^V \sum_{ip} \int^\Lambda \frac{d^3p}{(2\pi)^3} F(p) \tag{68}$$

is seen to be consistent with Eq. (30) after the Matsubara summation is carried out. The consistency of these equations with the original gap equation [Eq. (10)] can be achieved by adjusting the cutoff Λ. Thus, the second Ward identity (67) for the vertex $\Gamma_2^i(q)$ is fulfilled by the theory to the extent that the unknown cutoff is fixed by matching the gap functions obtained from finite range and contact interactions. We recall that the first identity for the vertex $\Gamma_1^i(q)$ is not satisfied to the extent that one uses the decoupling approximation and finite range integrations in deriving the normal self-energy.

VII. NEUTRINO EMISSIVITY

The neutrino emissivity (the power of the energy radiated per unit volume in neutrino-antineutrino pairs) is given by [2,21]

$$\begin{aligned} \epsilon_{\nu\bar{\nu}} &= -2 \left(\frac{G}{2\sqrt{2}}\right)^2 \int \frac{d^3q_1}{(2\pi)^3 2\omega_1} \int \frac{d^3q_2}{(2\pi)^3 2\omega_2} \int dq_0 \\ &\quad \times \int d^3\boldsymbol{q}\, \delta(\boldsymbol{q}_1 + \boldsymbol{q}_2 - \boldsymbol{q}) \delta(\omega_1 + \omega_2 - q_0)\, q_0 \\ &\quad \times g(q_0) \Lambda^{\mu\zeta}(q_1, q_2) \Im\mathrm{m}\, \Pi_{\mu\zeta}(q), \end{aligned} \tag{69}$$

where G is the weak coupling constant, $q_i = (\omega_i, \boldsymbol{q}_i)$, $i = 1, 2$ are the on-mass-shell four-momenta of neutrinos, $g(q_0) = [\exp(q_0/T) - 1]^{-1}$ is the Bose distribution function, $\Pi_{\mu\zeta}(q)$ is the retarded polarization tensor, $\Lambda^{\mu\lambda}(q_1, q_2) = \mathrm{Tr}[\gamma^\mu(1 - \gamma^5) \not{q}_1 \gamma^\nu (1 - \gamma^5) \not{q}_2]$. Here and below the emissivities are given per neutrino flavor; the total rate is obtained on multiplying the single flavor rate by the number of neutrino flavors within the standard model, $N_f = 3$.

The neutrino emissivity at one loop is obtained on substituting Eq. (18) into Eq. (69) and carrying out the phase-space integrals. The emissivity per neutrino flavor is then given by [1,2]

$$\epsilon_{\nu\bar{\nu}}^{1-\mathrm{loop}} = \epsilon_0 z^2 \int_{2z}^\infty dx \frac{x^5}{\sqrt{x^2 - 4z^2}} f\left(\frac{x}{2}\right)^2, \tag{70}$$

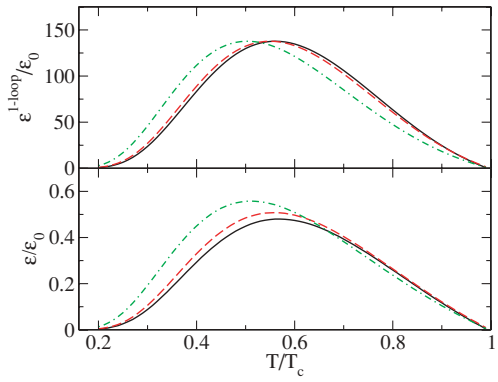

FIG. 5. (Color online) Dependence of neutrino emissivity in units of ϵ_0 for one-loop (upper panel) and full (lower panel) polarization tensor on the reduced temperature for Fermi wave vectors p_F (fm^{-1}) = 0.4 (solid), 0.8 (dashed, red online), and 1.4 (dashed-dotted, green online).

where $z = \Delta(T)/T$ and

$$\epsilon_0 = \frac{\nu(p_F) G^2 c_V^2}{60\pi^3} T^7. \tag{71}$$

However, the one-loop emissivity overestimates the true emission rate because the full and one-loop polarization tensors differ by the factor ξ_q/ω.

Although it is possible to obtain (numerically) the neutrino emissivity from the full polarization tensor without invoking the small-q expansion, we shall adopt the small q limit, because it permits us to obtain an analytical result. Thus we employ the $O(q^2)$ result given by Eq. (49) to obtain

$$\epsilon_{\nu\bar{\nu}} = \epsilon_0\, z^2 \frac{T}{m^*} \int_{2z}^\infty dx\, x^5\, f\left(\frac{x}{2}\right)^2. \tag{72}$$

Compared to the one-loop result the emissivity is suppressed by the factor T/m^*; this suppression is illustrated in Fig. 5. Note that the density dependence of the emissivities seen in Fig. 5 arises from the density dependence of the ratio $\Delta(T)/T$ as a function of T/T_c (in the BCS theory with contact interaction the ratio $\epsilon_{\nu\bar{\nu}}/\epsilon_0$ is universal). For $T \to T_c$ both rates vanish, consistent with the observation that the pair bremsstrahlung is absent in normal matter for on-shell baryons. At small $T \leqslant 0.3 T_c$ the rates are suppressed exponentially as $\exp(-\Delta/T)$. At intermediate temperatures the emissivity that includes vertex corrections is roughly by factor $\sim 5 \times 10^{-3}$ smaller than the its one-loop counterpart, in agreement with the qualitative estimate above.

VIII. SUMMARY AND OUTLOOK

We studied the modifications of the weak vector and axial-vector vertices in the nuclear medium by summing infinite series of irreducible particle-hole diagrams in terms of a contact (momentum and energy independent) driving interaction. These modification are cast into effective three-point vertex functions that are computed at finite temperatures, consistent with the finite temperature polarization function. We have clarified the relation between the vertex functions and the

self-energies implied by the generalized Ward identities. The renormalized vertices are implemented to compute the full polarization of matter and its expansion in small momentum transfer. The leading-order contribution to the polarization tensor is $O(q^2)$ consistent with the f-sum rule. This contribution is further used to obtain the neutrino losses via pair-breaking neutrino bremsstrahlung. We find neutrino loss rates that are suppressed compared to the one-loop results by a factor of order 5×10^{-3}. The magnitude of the suppression differs from the one predicted in Ref. [18] for reasons explained in the Introduction. The modifications to the neutrino emission rate through pair-breaking process found above call for a reassessment of their role in the late-time cooling of neutron stars. Preliminary estimates demonstrate that the neutrino emissivity via the pair-breaking processes in $^1S_0$ neutron superfluid is comparable to the emissivity of the competing modified pair-bremsstrahlung process [26].

Although we concentrated above on the neutral current interactions, our formalism can be adapted to compute the rates of neutrino emission beyond one loop for processes operating at higher densities within the cores of neutron stars. These include the charge-current Urca process $n \to p + e + \nu_e$ [52] and the charge-neutral current pair-braking process in the $^3P_2$-$^3F_2$ neutron superfluid and $^1S_0$ proton superconductor [11]. Vertex corrections could be important in the related problem of neutrino emission and propagation in quark matter [17], where one-loop results for a number of processes became available recently [53–58].

ACKNOWLEDGMENTS

We are grateful to S. Reddy for helpful communications and for drawing our attention to the sum rules. This work was, in part, supported by the Deutsche Forschungsgemainschaft through the SFB 382.

APPENDIX: MATSUBARA SUMS IN LOOPS

Here we quote the results for the loops and polarization tensors that have been used in the main text. The loops are defined as convolution products of the Matsubara Green's functions (here $\boldsymbol{k} = \boldsymbol{p} + \boldsymbol{q}$)

$$
\begin{aligned}
L_{GG}(q, \boldsymbol{p}) &= T \sum_{ip} G(ip, \boldsymbol{p}) G(ip + iq, \boldsymbol{k}) \\
&= \left(\frac{u_p^2 u_k^2}{iq + \epsilon_p - \epsilon_k} - \frac{v_p^2 v_k^2}{iq - \epsilon_p + \epsilon_k} \right) \\
&\quad \times [f(\epsilon_p) - f(\epsilon_k)] \\
&\quad + \left(\frac{u_k^2 v_p^2}{iq - \epsilon_p - \epsilon_k} - \frac{u_p^2 v_k^2}{iq + \epsilon_p + \epsilon_k} \right) \\
&\quad \times [f(-\epsilon_p) - f(\epsilon_k)], \qquad \text{(A1)}
\end{aligned}
$$

$$
\begin{aligned}
L_{FG}(q, \boldsymbol{p}) &= T \sum_{ip} F(ip, \boldsymbol{p}) G(ip + iq, \boldsymbol{k}) \\
&= -u_p v_p \left(\frac{u_k^2}{iq + \epsilon_p - \epsilon_k} + \frac{v_k^2}{iq - \epsilon_p + \epsilon_k} \right) \\
&\quad \times [f(\epsilon_p) - f(\epsilon_k)] \\
&\quad + u_p v_p \left(\frac{u_k^2}{iq - \epsilon_p - \epsilon_k} + \frac{v_k^2}{iq + \epsilon_p + \epsilon_k} \right) \\
&\quad \times [f(-\epsilon_p) - f(\epsilon_k)], \qquad \text{(A2)}
\end{aligned}
$$

$$
\begin{aligned}
L_{FF}(q, \boldsymbol{p}) &= T \sum_{ip} F(ip, \boldsymbol{p}) F^\dagger(ip + iq, \boldsymbol{k}) \\
&= u_p u_k v_p v_k \left\{ \left(\frac{1}{iq + \epsilon_p - \epsilon_k} - \frac{1}{iq - \epsilon_p + \epsilon_k} \right) \right. \\
&\quad \times [f(\epsilon_p) - f(\epsilon_k)] + \left(\frac{1}{iq + \epsilon_p + \epsilon_k} \right. \\
&\quad \left. \left. - \frac{1}{iq - \epsilon_p - \epsilon_k} \right) [f(-\epsilon_p) - f(\epsilon_k)] \right\}, \qquad \text{(A3)}
\end{aligned}
$$

$$
\begin{aligned}
L_{G^\dagger G}(q, \boldsymbol{p}) &= T \sum_{ip} G^\dagger(ip, \boldsymbol{p}) G(ip + iq, \boldsymbol{k}) \\
&= - \left(\frac{u_k^2 v_p^2}{iq + \epsilon_p - \epsilon_k} - \frac{u_p^2 v_k^2}{iq - \epsilon_p + \epsilon_k} \right) \\
&\quad \times [f(\epsilon_p) - f(\epsilon_k)] \\
&\quad - \left(\frac{u_p^2 u_k^2}{iq - \epsilon_p - \epsilon_k} - \frac{v_p^2 v_k^2}{iq + \epsilon_p + \epsilon_k} \right) \\
&\quad \times [f(-\epsilon_p) - f(\epsilon_k)], \qquad \text{(A4)}
\end{aligned}
$$

$$
\begin{aligned}
L_{FG^\dagger}(q, \boldsymbol{p}) &= T \sum_{ip} F(ip, \boldsymbol{p}) G^\dagger(ip + iq, \boldsymbol{k}) \\
&= u_p v_p \left(\frac{v_k^2}{iq + \epsilon_p - \epsilon_k} + \frac{u_k^2}{iq - \epsilon_p + \epsilon_k} \right) \\
&\quad \times [f(\epsilon_p) - f(\epsilon_k)] \\
&\quad - u_p v_p \left(\frac{v_k^2}{iq - \epsilon_p - \epsilon_k} + \frac{u_k^2}{iq + \epsilon_p + \epsilon_k} \right) \\
&\quad \times [f(-\epsilon_p) - f(\epsilon_k)]. \qquad \text{(A5)}
\end{aligned}
$$

The remainder loops are obtained from those defined above through the relations

$$
\begin{aligned}
L_{G^\dagger G^\dagger}(iq, \boldsymbol{p}) &= L_{GG}(-iq, \boldsymbol{p}), \\
L_{GF}(iq, \boldsymbol{p}) &= L_{FG}(-iq, \boldsymbol{p}), \qquad \text{(A6)} \\
L_{GG^\dagger}(iq, \boldsymbol{p}) &= L_{G^\dagger G}(-iq, \boldsymbol{p}), \\
L_{G^\dagger F}(iq, \boldsymbol{p}) &= L_{FG^\dagger}(-iq, \boldsymbol{p}), \qquad \text{(A7)}
\end{aligned}
$$

where, except for the first relation, we used the fact that the quasiparticle spectrum is reflection invariant, $\epsilon(-\boldsymbol{p}) = \epsilon(\boldsymbol{p})$. This property implies that the arguments of the functions can be interchanged $\boldsymbol{k} \leftrightarrow \boldsymbol{p}$ without changing the result. Furthermore,

on performing the substitution $\boldsymbol{p} \to -\boldsymbol{p} - \boldsymbol{q}$ one finds that

$$L_{GG}(iq, \boldsymbol{p}) = L_{G^\dagger G^\dagger}(iq, \boldsymbol{p}), \quad L_{GF}(iq, \boldsymbol{p}) = L_{FG^\dagger}(iq, \boldsymbol{p}),$$
$$L_{FG}(iq, \boldsymbol{p}) = L_{G^\dagger F}(iq, \boldsymbol{p}). \tag{A8}$$

The retarded polarization tensor is obtained by analytical continuation in the loops $L_{XX'}(iq, \boldsymbol{p}) = L_{XX'}(\omega + i\delta, \boldsymbol{p})$ and by subsequent integration over the three-momentum $\boldsymbol{p}$ according to Eq. (25).

[1] E. G. Flowers, M. Ruderman, and P. G. Sutherland, Astrophys. J. **205**, 541 (1976).
[2] D. N. Voskresensky and A. V. Senatorov, Sov. J. Nucl. Phys. **45**, 411 (1987) [Yad. Fiz. **45**, 657 (1987)]; A. B. Migdal, E. E. Saperstein, M. A. Troitsky, and D. N. Voskresensky, Phys. Rep. **192**, 179 (1990).
[3] Ch. Schaab, D. N. Voskresensky, A. Sedrakian, F. Weber, and M. K. Weigel, Astron. Astrophys. **321**, 591 (1997).
[4] S. Tsuruta, M. A. Teter, T. Takatsuka, T. Tatsumi, and R. Tamagaki, Astrophys. J. **571**, L143 (2002).
[5] D. Blaschke, H. Grigorian, and D. N. Voskresensky, Astron. Astrophys. **424**, 979 (2004).
[6] D. Page, J. M. Lattimer, M. Prakash, and A. W. Steiner, Astrophys. J. Suppl. **155**, 623 (2004).
[7] H. Grigorian and D. N. Voskresensky, Astron. Astrophys. **444**, 913 (2005).
[8] V. A. Khodel, J. W. Clark, M. Takano, and M. V. Zverev, Phys. Rev. Lett. **93**, 151101 (2004).
[9] D. N. Voskresensky, *Lecture Notes in Physics* (Springer-Verlag, New York, 2001), Vol. 578, p. 467.
[10] A. Sedrakian, Prog. Part. Nucl. Phys. **58**, 168 (2007), eprint nucl-th/0601086.
[11] A. D. Kaminker, P. Haensel, and D. G. Yakovlev, Astron. Astrophys. **345**, L14 (1999); L. B. Leinson, Nucl. Phys. **A687**, 489 (2001); D. G. Yakovlev, A. D. Kaminker, and K. P. Levenfish, Astron. Astrophys. **343**, 650 (1999).
[12] Y. Nambu, Phys. Rev. **117**, 648 (1960).
[13] J. R. Schrieffer, *Theory of Superconductivity* (Benjamin, New York, 1964).
[14] A. Leggett, Phys. Rev. **147**, 119 (1966).
[15] A. B. Migdal, *Theory of Finite Fermi Systems and Applications to Atomic Nuclei* (Interscience, London, 1967).
[16] P. Ring and P. Schuck, *The Nuclear Many Body Problem* (Springer-Verlag, New York, 1980).
[17] J. Kundu and S. Reddy, Phys. Rev. C **70**, 055803 (2004).
[18] L. B. Leinson and A. Pérez, Phys. Lett. **B638**, 114 (2006).
[19] The small-q expansion of the matrix elements in Eq. (17) of Ref. [18] leads to $O(q)$ contributions that are not suppressed by factors v_F/c. These contributions were omitted in Ref. [18] by approximating the Bogolyubov amplitudes as $u_{p+q} \simeq u_p$ and $v_{p+q} \simeq v_p$, where q is the transfered momentum.
[20] O. V. Maxwell and B. L. Friman, Astrophys. J. **232**, 541 (1979).
[21] A. Sedrakian and A. E. L. Dieperink, Phys. Lett. **B463**, 145 (1999); Phys. Rev. D **62**, 083002 (2000); A. Sedrakian, arXiv:astro-ph/0701017.
[22] C. Hanhart, D. R. Phillips, and S. Reddy, Phys. Lett. **B463**, 9 (2001).
[23] E. N. E. van Dalen, A. E. L. Dieperink, and J. A. Tjon, Phys. Rev. C **67**, 065807 (2003).
[24] R. G. E. Timmermans, A. Yu. Korchin, E. N. E. van Dalen, and A. E. L. Dieperink, Phys. Rev. C **65**, 064007 (2002).
[25] A. Schwenk, P. Jaikumar, and C. Gale, Phys. Lett. **B584**, 241 (2004).
[26] A. Sedrakian and J. W. Clark, in *Recent Progress in Many-Body Theories 14* (World Scientific, Singapore, in press); arXiv:0710.0779 [nucl-th].
[27] D. Pines and C. Pethick, in *Proceedings of the XIth International Conference on Low Temperature Physics*, edited by E. Kandu (Kligatu, Tokyo, 1971).
[28] J. W. Clark, C. G. Källman, C. H. Yang, and D. A. Chakkalakal, Phys. Lett. **B61**, 331 (1976).
[29] J. M. C. Chen, J. W. Clark, E. Krotscheck, and R. A. Smith, Nucl. Phys. **A451**, 509 (1986).
[30] J. M. C. Chen, J. W. Clark, R. D. Davé, and V. V. Khodel, Nucl. Phys. **A555**, 59 (1993).
[31] J. Wambach, T. L. Ainsworth, and D. Pines, Nucl. Phys. **A555**, 128 (1993).
[32] H.-J. Schulze, J. Cgunon, A. Lejune, M. Baldo, and U. Lombardo, Phys. Lett. **B375**, 1 (1996).
[33] A. Sedrakian, Phys. Rev. C **68**, 065805 (2003).
[34] A. Schwenk, B. Friman, and G. Brown, Nucl. Phys. **A713**, 191 (2003); K. Hebeler, A. Schwenk, and B. Friman, Phys. Lett. **B648**, 176 (2007).
[35] C. Shen, U. Lombardo, P. Schuck, W. Zuo, and N. Sandulescu, Phys. Rev. C **67**, 061302(R) (2003).
[36] A. Fabrocini, S. Fantoni, A. Y. Illarionov, and K. E. Schmidt, Phys. Rev. Lett. **95**, 192501 (2005).
[37] C. Shen, U. Lombardo, and P. Schuck, Phys. Rev. C **71**, 054301 (2005).
[38] H. Müther and W. H. Dickhoff, Phys. Rev. C **72**, 054313 (2005).
[39] U. Lombardo and H.-J. Schulze, *Lecture Notes in Physics* (Springer-Verlag, New York, 2001), Vol. 578, p. 30.
[40] D. J. Dean and M. Hjorth-Jensen, Rev. Mod. Phys. **75**, 607 (2003).
[41] A. Sedrakian and J. W. Clark, *Pairing in Fermionic Systems: Basic Concepts and Modern Applications* (World Scientific, Singapore, 2007), Chap. 6.
[42] A. A. Abrikosov, L. P. Gorkov, and I. E. Dzyaloshinkski, *Methods of Quantum Field Theory in Statistical Physics* (Dover, New York, 1975).
[43] In the common notation these quantities correspond to the f and g Landau parameters;the present notation anticipates that these constants are the driving terms in the vector and axial-vector channels.
[44] W. H. Dickhoff, A. Faessler, J. Meyer-ter-Vehn, and H. Müther, Phys. Rev. C **23**, 1154 (1981).
[45] R. Machleidt, Phys. Rev. C **63**, 024001 (2001).
[46] A. Sedrakian and J. W. Clark, Phys. Rev. C **73**, 035803 (2006).
[47] A. Sedrakian, T. T. S. Kuo, H. Müther, and P. Schuck, Phys. Lett. **B576**, 68 (2003).
[48] U. Lombardo, P. Schuck, and W. Zuo, Phys. Rev. C **64**, 021301(R) (2001).
[49] J. Kuckei, F. Montani, H. Müther, and A. Sedrakian, Nucl. Phys. **A723**, 32 (2003).
[50] A. Sedrakian, T. Alm, and U. Lombardo, Phys. Rev. C **55**, R582 (1997); A. Sedrakian and U. Lombardo, Phys. Rev. Lett. **84**, 602 (2000); U. Lombardo, P. Nozières, P. Schuck, H.-J. Schulze, and A. Sedrakian, Phys. Rev. C **64**, 064314 (2001); A. I. Akhiezer, A. A. Isayev, S. V. Peletminsky, and A. A. Yatsenko, *ibid.* **63**, 021304 (2001); A. Sedrakian, *ibid.* **63**, 025801 (2001); A. A. Isayev, *ibid.* **65**, 031302 (2002).

[51] J. W. Negele and H. Orland, *Quantum Many-Particle Systems* (Westview Press, Boulder, 1998).
[52] A. Sedrakian, Phys. Lett. **B607**, 27 (2005).
[53] P. Jaikumar, C. D. Roberts, and A. Sedrakian, Phys. Rev. C **73**, 042801(R) (2006).
[54] Q. Wang, Z. G. Wang, and J. Wu, Phys. Rev. D **74**, 014021 (2006); Q. Wang, eprint hep-ph/0607096.
[55] A. Schmitt, I. A. Shovkovy, and Q. Wang, Phys. Rev. D **73**, 034012 (2006).
[56] M. G. Alford and A. Schmitt, J. Phys. G **34**, 67 (2007).
[57] B. A. Sa'd, I. A. Shovkovy, and D. H. Rischke, Phys. Rev. D **75**, 065016 (2007).
[58] R. Anglani, G. Nardulli, M. Ruggieri, and M. Mannarelli, Phys. Rev. D **74**, 074005 (2006); R. Anglani, arXiv:hep-ph/0610404.